JOURNAL OF THEORETICAL
AND APPLIED MECHANICS
4, 38, 2000

STABILITY OF INCOMPRESSIBLE ATTACHMENT-LINE BOUNDARY LAYER

EWA TULISZKA-SZNITKO
MARIUSZ WRONA

Institute of Thermal Engineering, Technical University of Poznań
e-mail: sznitko@put.poznan,pl

Linear stability analysis of incompressible attachment-line flow is presented within temporal and special frameworks. The global solution method used for solving the eigenproblem yields a full spectrum of the least damped waves. Analyses are made for the cases with blowing and suction. The equations of linear stability theory are solved using the spectral collocation method. The results obtained are compared with those presented by Hall (1984), Spalart (1988) and Theofilis (1998) and with the available experimental data.

Key words: instability, attachment-line boundary layer

1. Introduction

Recent studies a special advanced technology project such as a laminar flow around the aircraft have highlighted the importance of the flow in the vicinity of swept leading edge and in particular at the attachment-line. The research aims at minimisation drag and hence reduction of fuel consumption using suction to control the development of the laminar wing boundary layer and delay the transition to turbulence. Many instability mechanisms may aris which cause the breakdown of laminar flow to the turbulent one on swept wings. Among others, the laminar-turbulent transition on a swept wing can be caused by crossflow instability, Tollmien-Schlichting waves, Görtler vortices and the instability of attachment-line.

The present consideration will focus on those disturbances which evolve close to the attachment-line region. The boundary layer which develops along the swept attachment-line can be either laminar or turbulent. There are two

main ways of transition from the laminar to turbulent flow. The first one arises if the attachment-line is contaminated by turbulent structures originating from the fuselage. In this case the boundary layer can be turbulent directly at the attachment-line which is unfavourable from the technological point of view. The leading edge contamination is a fully nonlinear phenomenon of "bypass" type. The leading edge contamination may occur when the Reynolds number exceeds a value about $\mathrm{Re} = 250$, where

$$\mathrm{Re} = \frac{W_\infty \Delta}{\nu} \tag{1.1}$$

and

W_∞	–	free-stream spanwise velocity (Fig.1)
Δ	–	length scale, $\Delta = \sqrt{\nu/(dU_e/dx)}$
dU_e/dx	–	velocity gradient at the attachment-line
ν	–	kinematic viscosity.

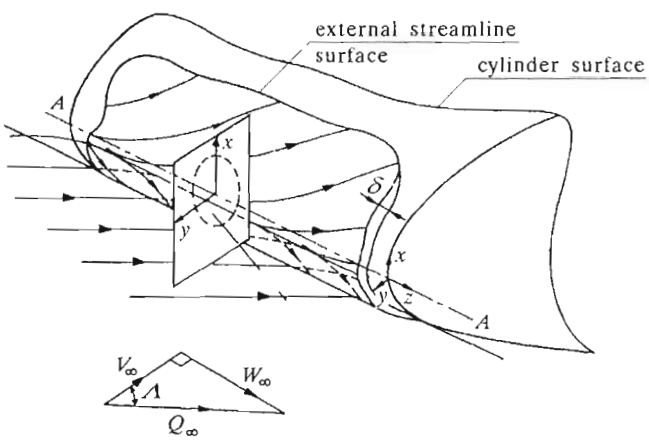

Fig. 1. Scheme of the attachment-line boundary layer, Theofilis (1998)

The leading edge contamination will not be investigated in this paper.

If the swept model is not in contact with a solid surface (Fig.2) we deal with the so called "natural" transition (second way). In such a case the laminar boundary layer starts to develop at the point A (Fig.2). The transition results from amplification of the disturbances inside the boundary layer which are generated by small disturbances in the free-stream flow. This situation arises in the swept wing flow if the leading edge contamination is avoided by suction.

The problem of the attachment-line instability has been considered by many authors. Gaster (1967) was the first who investigated experimentally the small-amplitude development by using acoustic excitation along the

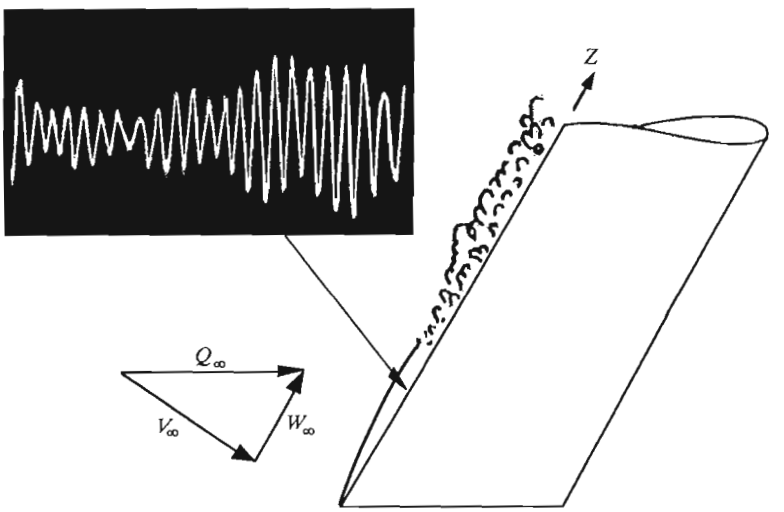

Fig. 2. "Natural" transition on a swept model and hot wire records, Pfenninger and Bacon (1969)

attachment-line of a swept cylinder. He concluded that the small-amplitude disturbances in the attachment-line boundary layer were stable for the momentum-thickness Reynolds number Re_Θ not exceeding 170 ($\mathrm{Re} = 420$). Pfenninger and Bacon (1969) used a 45° swept wing to study the attachment-line instabilities in a wind tunnel and they observed regular sinusoidal oscillations (Fig.2) at the frequencies comparable to those appearing at most unstable 2D modes of the theory. Poll (1979, 1985) performed many experiments with the attachment-line of swept wing. He concluded that in a quiet environment with a smooth surface (natural transition) the attachment-line remained laminar up to $\mathrm{Re} = 570$. The hot wire measurements showed that the 2D disturbances developed in the attachment-line boundary layers and that the whole laminar-turbulent transition process was very similar to that observed in the 2D boundary layers.

Theoretically, Poll (1979) predicted the critical Reynolds number Re_{cr} to be 670 using the linear parallel stability theory. Then Hall et al. (1984) obtained Re_{cr} of 583 which was very close to the experimental results of 570. They used the non-parallel stability theory for the generalised Hiemenz flow within the so-called Görtler-Hammerlin framework. This result was confirmed by Spalart (1988) who made direct simulation of the flow near the attachment line of a swept cylindrical body by solving numerically (DNS) the full Navier-Stokes equations. Lin and Malik (1996) considered the general three-dimensional di-

sturbances whose eigenfunctions depended on the normal and chordwise coordinates. They confirmed that the dominant instability was that analysed by Hall et al. (1984). Stability of the incompressible swept attachment-line boundary layer was studied by Theofilis (1998) within the Görtler-Hammerlin framework, in both linear and nonlinear two-dimensional regimes. He showed that the linear initial-boundary-value problem formulation yielded results being in excellent agreement with the results obtained by the use of linear stability theory. Balakumar (1998) computed the 2D nonlinear equilibrium solutions for the swept Hiemenz flow attachment-line boundary layer by solving the full Navier-Stokes equations as a nonlinear eigenvalue problem. He found that the nonlinear critical point occured at the Reynolds number of 511. Bertolotti (1999) analysed the relation between the attachment-line instability and crossflow instability.

In this paper we investigate the stability of the incompressible swept attachment-line boundary layer within the Görtler-Hammerlin framework. The equations of linear non-parallel stability theory create an eigenvalue problem which is solved in a global manner; the global approach allows for recovery of the full spectrum of eigenmodes not only the most unstable one. Calculations are performed for zero suction and for the boundary layers in which blowing and suction are applied to demonstration of the possibility of controlling the attachment-line boundary layer. Our results are compared with the results obtained by Hall et al. (1984), Spalart (1988), Theofilis (1998) and with the experimental data of Pfenninger and Bacon (1969), Poll (1979) and Powilleit (1992). In this paper we collected the results of research into the attachment-line instability obtained by different authors taking different approaches. The aim was to check the accuracy of our results as well as to justify the use of the Görtler-Hammerlin form of disturbances in this and planed work.

2. Basic state equations

We consider the attachment-line boundary layer at long distances from its origin (point A in Fig.2). Pfenninger and Bacon (1969) showed that the parallel boundary layer could be reached even within a small spanwise distance from point A so that, it can be assumed that the main properties of the basic state (shape factor, skin friction coefficient, integral thickness are constant) do not depend on the spanwise location at long distances from its origin. For this kind of flow it is possible to obtain the exact solution of the incompressible Navier-Stokes equations (which is the so-called generalised Hiemenz flow).

In the paper we consider the incompressible viscous flow over an infinite flat plate which is located at $y = 0$ in the Cartesian co-ordinate system $(x, y, z$; Fig.1). The x-axis coincides with the chord direction, y-axis is normal to the plate and z-axis overlaps the attachment-line. The velocity components are u, v and w.

The inviscid velocity distributions for this flow are defined as

$$U_e = \frac{U_0 x}{l} \qquad W_e = W_0 = \text{const} \tag{2.1}$$

where l is the length scale in the x direction and U_0, W_0 are the independent velocity scales. We seek for a similarity solution of the following form

$$u = U_0\Big(\frac{x}{l}\Big)\overline{u}(\eta) \qquad v = U_0\Big(\frac{\Delta}{l}\Big)\overline{v}(\eta) \qquad w = W_0\overline{w}(\eta) \tag{2.2}$$

where $\eta = y/\Delta$. Substituting these structures into the incompressible Navier-Stokes equations we obtain the system of ordinary differential equations

$$\begin{aligned} &\overline{u} + \overline{v}' = 0 \\ &\overline{v}''' + (\overline{v}')^2 - \overline{v}\overline{v}'' - 1 = 0 \\ &\overline{w} + \overline{v}\overline{w}' = 0 \end{aligned} \tag{2.3}$$

The boundary conditions are

$$\begin{aligned} &\overline{v}(0) = \kappa \qquad \overline{v}'(0) = 0 \qquad \overline{w}(0) = 0 \\ &\overline{v}'(\infty) = -1 \qquad \overline{w}(\infty) = 1 \end{aligned} \tag{2.4}$$

In the above equations κ denotes the non-dimensional parameter used for suction control in the attachment-line boundary layer. The obtain the velocity profiles the non-linear systems of equations (2.3) with boundary conditions (2.4) is solved iteratively using the fourth order Runge-Kutta method. To solve above system of equations iteratively the very precise first assumption for $\overline{v}''$ and $\overline{w}'$ at the wall is necessary. For $\kappa = 0$ we have: $\overline{v}''(0) = -1.23258765$, $\overline{w}'(0) = 0.57046525$. For more details of the generalised swept Hiemenz solution, the Readers are referred to Rosenhead (1963).

The velocity profiles $\overline{u}, \overline{w}, \overline{v}$ and their first derivative obtained for $\kappa = 0$ are shown in Fig.3. The main characteristic values of the two boundary layers (in x and z directions) are: displacement thickness $\delta_x = 0.6479004743977949$, $\delta_z = 1.026227542367512$, momentum thickness $\Theta_x = 0.2923435912116265$, $\Theta_z = 0.4042302941011554$ and shape factor $H_x = 2.216229443281285$, $H_z = 2.538720025052618$. These integral quantities have been used to check accuracy of the obtained basic state profiles.

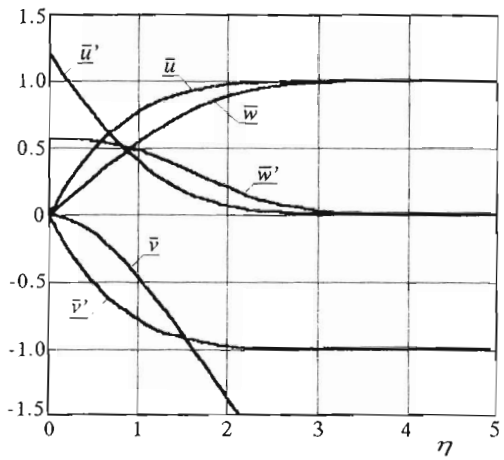

Fig. 3. Basic state profiles. The velocity profiles $\overline{u}, \overline{v}, \overline{w}$ and their first derivative obtained for $\kappa = 0$

3. Perturbed flow

In the perturbed flow analysis all the parameters are nondimensionalized:
— velocity components u, v and w by W_e

$$u = W_e U(X,Y,Z,t) \qquad v = W_e V(X,Y,Z,t)$$
$$w = W_e W(X,Y,Z,t) \tag{3.1}$$

— pressure p by ρW_e^2

$$p = \rho W_e^2 P(X,Y,Z,t) \tag{3.2}$$

The co-ordinates x, y and z are nondimensionalized by Δ

$$x = \Delta X \qquad y = \Delta\eta = \Delta Y \qquad z = \Delta Z \tag{3.3}$$

The disturbance equations are obtained by representing the velocity and pressure fields as a superposition of the basic and perturbation flows. The simplest idea is to introduce disturbances of the Tollmien-Schlichting waves form. The linear Tollmien-Schlichting disturbances are of the form

$$\{U', V', W', P'\}(Y,Z,t) = \{\widehat{u}, \widehat{v}, \widehat{w}, \widehat{p}\}(Y) e^{i(\beta Z - \omega t)} \tag{3.4}$$

The parallel flow approximation is then applied and finally we obtain the fourth-order Orr-Sommerfeld equation written for the attachment line profile $\overline{w}$. In such an approach the Orr-Sommerfeld equation describes the development of small disturbances in the attachment-line boundary layer.

It is possible to follow a more rigorous approach by considering a special class of disturbances, first introduced by Hammerlin (1955) and Görtler (1955). Following Hammerlin and Görtler we assume that the perturbations U', V', W' and P' are functions of Y and Z, however, the velocity in the chordwise direction varies linearly with X

$$
\begin{aligned}
U &= \frac{1}{\mathrm{Re}} X\overline{u}(Y) + XU'(Y,Z,t) \\
W &= \overline{w}(Y) + W'(Y,Z,t) \\
V &= \frac{1}{\mathrm{Re}}\overline{v}(Y) + V'(Y,Z,t) \\
P &= -\frac{1}{2\mathrm{Re}^2}X^2 + \frac{1}{\mathrm{Re}^2}P_0(Y) + P'(Y,Z,t)
\end{aligned}
\tag{3.5}
$$

We substitute the above equations into a non-dimensional form of the incompressible Navier-Stokes equations and the continuity equation.

$$
\begin{aligned}
&\boldsymbol{V}_t + (\boldsymbol{V}\cdot\nabla)\boldsymbol{V} = -\nabla P + \frac{1}{\mathrm{Re}}\nabla^2\boldsymbol{V} \\
&\nabla\cdot\boldsymbol{V} = 0
\end{aligned}
\tag{3.6}
$$

where $\boldsymbol{V}(U,V,W)$ is the velocity vector. After substituting Eqs (3.5) into the Navier-Stokes equations, eliminating pressure by cross differentiation and subtracting of the basic state we obtain the system of partial differential equations

$$
\begin{aligned}
&U' + \frac{\partial V'}{\partial Y} + \frac{\partial W'}{\partial Z} = 0 \\
&\frac{\partial^2 U'}{\partial Y^2} + \frac{\partial^2 U'}{\partial Z^2} - \mathrm{Re}\frac{\partial U'}{\partial t} - \mathrm{Re}\overline{w}\frac{\partial U'}{\partial Z} - \overline{v}\frac{\partial U'}{\partial Y} - 2\overline{u}U' - \frac{\partial\overline{u}}{\partial Y}V' = \\
&= \mathrm{Re}\Big(U'^2 + V'\frac{\partial U'}{\partial Y} + W'\frac{\partial U'}{\partial Z}\Big) \\
&\frac{\partial^3 W'}{\partial Y^3} + 2\frac{\partial^3 W'}{\partial Y\partial Z^2} - \mathrm{Re}\frac{\partial^2 W'}{\partial Y\partial t} - \mathrm{Re}\overline{w}\frac{\partial^2 W'}{\partial Y\partial Z} - \frac{\partial\overline{v}}{\partial Y}\frac{\partial W'}{\partial Y} - \overline{v}\frac{\partial^2 W'}{\partial Y^2} +
\end{aligned}
\tag{3.7}
$$

$$+\mathrm{Re}\frac{\partial\overline{w}}{\partial Y}U' - \mathrm{Re}\frac{\partial^2\overline{w}}{\partial Y^2}V' + \frac{\partial^2 U'}{\partial Y\partial Z} - \frac{\partial^3 V'}{\partial Z^3} + \mathrm{Re}\frac{\partial^2 V'}{\partial Z\partial t} + \mathrm{Re}\overline{w}\frac{\partial^2 V'}{\partial Z^2} +$$
$$-\overline{v}\frac{\partial W'}{\partial Z} - \overline{v}\frac{\partial^2 W'}{\partial Z^2} + \frac{\partial\overline{v}}{\partial Y}\frac{\partial V'}{\partial Z} = \mathrm{Re}\Big(-U'\frac{\partial W'}{\partial Y} + V'\frac{\partial^2 W'}{\partial Y^2} +$$
$$+W'\frac{\partial^2 W'}{\partial Y\partial Z} + U'\frac{\partial V'}{\partial Z} + V'\frac{\partial U'}{\partial Z} + V'\frac{\partial^2 W'}{\partial Z^2} - W'\frac{\partial^2 V'}{\partial Z^2}\Big)$$

We can seek for the solution of the above equations in the form of Fourier series (such an approach was used by Balakumar (1998) and Herbert (1977))

$$\{U', V', W', P'\}(Y, Z, t) = \sum_{n=-\infty}^{n=\infty} \{\widehat{u}_n, \widehat{v}_n, \widehat{w}_n, \widehat{p}_n\}(Y)\mathrm{e}^{\mathrm{i}(\beta Z - n\omega t)} \tag{3.8}$$

In this paper we pay our attention only to the linear stability of the flow (2.3). As for the Tollmien-Schlichting waves, the amplitudes $\widehat{u}, \widehat{v}, \widehat{w}, \widehat{p}$ of disturbances read

$$\{U', V', W', P'\}(Y, Z, t) = \{\widehat{u}, \widehat{v}, \widehat{w}, \widehat{p}\}(Y)\mathrm{e}^{\mathrm{i}(\beta Z - \omega t)} \tag{3.9}$$

The X-dependence of the disturbances in Eq (3.5) does not seem justified at first sight. Hammerlin and Görtler chose it for the reason of "mathematical feasibility". The X-dependence of the disturbance enables one to find a solution of the linear stability equations by solving ordinary differential equations. In most cases the non-parallel linear stability analysis leads to a partial differential system. However, recent investigations performed by Spalart (1988) by using the direct method confirmed the Görtler-Hammerlin assumption in the sense that the disturbances of (3.5) are most unstable and therefore the most relevant in stability studies.

After introducing Eq (3.9) into the disturbance equations (3.7), linearizing in $\widehat{u}, \widehat{v}, \widehat{w}$ and after some transformations we obtain the following system of equations

$$\begin{aligned}
&(D^2 - \overline{v}D - \beta^2 - 2\overline{u} - \mathrm{i}\beta\mathrm{Re}\overline{w})\widehat{u} - (D\overline{u})\widehat{v} = -\mathrm{iRe}\omega\widehat{u} \\
&[2(D\overline{u}) + 2\overline{u}D]\widehat{u} + \Big\{D^4 - \overline{v}D^3 + [-2\beta^2 - \mathrm{i}\beta\mathrm{Re}\overline{w} - (D\overline{v})]D^2 + \\
&+[\beta^2\overline{v} + (D\overline{u})]D + \beta^4 + \mathrm{i}\beta^3\mathrm{Re}\overline{w} + \mathrm{i}\beta\mathrm{Re}(D^2\overline{w}) + \\
&+\beta^2(D\overline{v}) + (D^2\overline{u})\Big\}\widehat{v} = -\mathrm{iRe}\omega(D^2 - \beta^2)\widehat{v}
\end{aligned} \tag{3.10}$$

where $D = d/dY$.

The boundary conditions associated with the system to be solved deserve some discussion. In the perturbation equations at the wall the viscous condition of zero perturbations is imposed on $\widehat{u}, \widehat{v}$ and zero derivative for the normal perturbation velocity

$$\widehat{u} = \widehat{v} = D\widehat{v} = 0 \qquad Y = 0 \tag{3.11}$$

In the far-field, condition of vanishing perturbations at a sufficiently long distance from the wall may be imposed

$$\widehat{u} = \widehat{v} = D\widehat{v} = 0 \qquad Y \to 0 \tag{3.12}$$

or the asymptotic solution of Eqs (3.10) in the limit passage $\overline{w}(\infty) = 1$, $D\overline{v}(\infty) = -1$, $\overline{u}(\infty) = 1$ may be utilised. Eqs (3.10) as $Y \to \infty$ can be written in the following way

$$[D^2 + (Y-\delta)D - \beta^2 - 2 - \mathrm{i}\beta\mathrm{Re}]\widehat{u} = -\mathrm{iRe}\omega\widehat{u}$$

$$2D\widehat{u} + \Big\{D^4 + (Y-\delta)D^3 + [-2\beta^2 - \mathrm{i}\beta\mathrm{Re} + 1]D^2 - \beta^2(Y-\delta)D + \beta^4 + \tag{3.13}$$

$$+\mathrm{i}\beta^3\mathrm{Re} - \beta^2(Y-\delta)\Big\}\widehat{v} = -\mathrm{iRe}\omega(D^2 - \beta^2)\widehat{v}$$

where δ is the boundary layer thicknes. Hall et al. (1984) looked for asymptotic solutions of Eq (3.13) and he found that $\widehat{u}, \widehat{v}$ are to decay expotentially as $Y \to \infty$

$$\widehat{u} \sim \mathrm{e}^{-\frac{1}{2}Y^2} \qquad \widehat{v} \sim \mathrm{e}^{-\beta Y} \tag{3.14}$$

We note that the velocity component $\widehat{v}$ tends to zero more slowly than $\widehat{u}$.

Eqs (3.10) with boundary conditions (3.11) and (3.12) create, of course, an eigenvalue problem. However, in contrast with the Orr-Sommerfeld approach, Eq (3.10) are obtained without using a parallel flow approximation. In other words, the Görtler-Hammerlin waves are an exact solution of the linearized Navier-Stokes equations. Let us recall that the basic state profiles are obtained from Eqs (2.3) which is a solution of the full Navier-Stokes equations, not just of the boundary layer equations. We can expect that such an approach gives a very accurate description of small disturbances development in a linear part of the laminar-turbulent transition region.

4. Numerical approach

Eqs (3.10) and boundary conditions (3.11), (3.12) create the generalised

eigenvalue problem which within the framework of temporal theory (complex ω and real β) can be written in the following form

$$\mathbf{A}\Psi = \omega \mathbf{B}\Psi \tag{4.1}$$

where $\Psi = [\widehat{u}, \widehat{v}]^{\top}$.

Within the framework of the spatial theory (real ω and complex β) the eigenvalue problem resulting from Eqs (3.10)$\div$(3.12) is strongly non-linear. To linearize the eigenvalue problem we introduce new variables: $\beta\widehat{u}, \beta\widehat{v}, \beta^2\widehat{v}, \beta^3\widehat{v}$. Within the framework of the spatial theory the generalised eigenvalue problem can be written as follows

$$\mathbf{A}\Psi = \beta \mathbf{B}\Psi \tag{4.2}$$

where $\Psi = [\widehat{u}, \beta\widehat{u}, \widehat{v}, \beta\widehat{v}, \beta^2\widehat{v}, \beta^3\widehat{v}]^{\top}$.

The spectral method based on the Chebyshev polynomials has been used to obtain a solution of high accuracy to the linear stability theory. The most important feature of the spectral method is exponential convergence which allows for attaining a high degree accuraty with a modest number of collocation points $N = 30 \div 70$. Accuracy is, of course, of primary importance in stability analysis however, it is of particular interest when the global approach is taken which yields a full eigenvalue spectrum. It is much more difficult to obtain the full spectrum (if possible at all) than to solve the local problem in which we estimate only the most unstable eigenvalue. Perhaps alternatively to descretise Eq (3.10) one could use the fourth order accurate two-point scheme, which is derived by means of the Euler-Maclurin formula. This scheme was not used in the present paper since it has already been applied to the attachment-line instability analysis by Hall et al. (1984) and Balakumar (1998). The grid refinement histories of the numerical solution of the eigenvalue problem obtained in the present paper with the spectral collocation method and that obtained by Hall et al. (1984) with the Euler-Maclurin formula are analysed in Section 5.

In the considered case the swept attachment-line boundary layer flow, the physical domain $Y \in (0, \infty)$ has to be mapped onto the standard spectral collocation domain $\overline{y} \in (-1, 1)$ by the function

$$Y_j = \frac{a(1 + \overline{y}_j)}{b - \overline{y}_j} \tag{4.3}$$

where

$$a = \frac{Y_0 Y_{max}}{Y_{max} - 2Y_0} \qquad b = 1 + \frac{2a}{Y_{max}} \tag{4.4}$$

Y_0 is chosen to divide the domain in to two with the same number of collocation points, Y_{max} is the location where the calculation domain for the basic flow

is truncated. The derivative matrices $\widehat{D}^m_{i,j}$ in $Y \in (0,\infty)$ domain have to be obtained from the following equations

$$\begin{aligned}
\widehat{D}^{(1)}_{i,j}(Y) &= \frac{d\overline{y}}{dY} D^{(1)}_{i,j}(\overline{y}) \\
\widehat{D}^{(2)}_{i,j}(Y) &= \Big(\frac{d\overline{y}}{dY}\Big)^2 D^{(2)}_{i,j}(\overline{y}) + \frac{d^2\overline{y}}{dY^2} D^{(1)}_{i,j}(\overline{y}) \\
\widehat{D}^{(3)}_{i,j}(Y) &= \Big(\frac{d\overline{y}}{dY}\Big)^3 D^{(3)}_{i,j}(\overline{y}) + 3\frac{d^2\overline{y}}{dY^2}\frac{d\overline{y}}{dY} D^{(2)}_{i,j}(\overline{y}) + \frac{d^3\overline{y}}{dY^3} D^{(1)}_{i,j}(\overline{y}) \\
\widehat{D}^{(4)}_{i,j}(Y) &= \Big(\frac{d\overline{y}}{dY}\Big)^4 D^{(4)}_{i,j}(\overline{y}) + 6\frac{d^2\overline{y}}{dY^2}\Big(\frac{d\overline{y}}{dY}\Big)^2 D^{(3)}_{i,j}(\overline{y}) + 3\Big(\frac{d^2\overline{y}}{dY^2}\Big)^2 D^{(2)}_{i,j}(\overline{y}) + \\
&\quad + 4\frac{d^3\overline{y}}{dY^3}\frac{d\overline{y}}{dY} D^{(2)}_{i,j}(\overline{y}) + \frac{d^4\overline{y}}{dY^4} D^{(1)}_{i,j}(\overline{y})
\end{aligned} \tag{4.5}$$

where $D^{(m)}_{i,j}$ is the matrix which performs collocation differentiation in the basic Chebyshev domain $\overline{y} \in [-1,1]$ (Theofilis, 1985). Values of first derivative matrix $D^{(1)}_{i,j}$ are obtained as follows (Canuto et al., 1988)

$$D^{(1)}_{i,j} = \begin{cases} \dfrac{2N^2+1}{6} & j = i = 0 \\ -\dfrac{x_j}{2(1-x_j^2)} & j = i \\ \dfrac{\overline{c}_i(-1)^{j+i}}{\overline{c}_j(\overline{y}_i - \overline{y}_j)} & j \neq i \\ -\dfrac{2N^2+1}{6} & j = i = N \end{cases} \tag{4.6}$$

where

$$\overline{c}_j = \begin{cases} 2 & j = 0 \\ 1 & 1 \leqslant j \leqslant N-1 \\ 2 & j = N \end{cases}$$

and N is the number of collocations points. Higher derivatives can be obtained by the repeated application of $D^{(1)}_{i,j}$. The elements of matrixes **A** and **B** in Eq (4.1) (temporal approach) can be written as follows:

— for $i = j$

$$\mathbf{a}_{i,j} = \begin{bmatrix} \widehat{D}^{(2)}_{i,j} - \overline{v}_i \widehat{D}_{i,j} - \beta^2 + & -\widehat{D}_{i,j}\overline{u}_i \\ -2\overline{u}_i - \mathrm{i}\beta\mathrm{Re}\overline{w}_i & \\ & \\ 2(\widehat{D}_{i,j}\overline{u}_i) + 2\overline{u}_i\widehat{D}_{i,j} & \widehat{D}^{(4)}_{i,j} - \overline{v}_i\widehat{D}^{(3)}_{i,j} + \\ & +[-2\beta^2 - \mathrm{i}\beta\mathrm{Re}\overline{w}_i - (\widehat{D}_{i,j}\overline{v}_i)]\widehat{D}^{(2)}_{i,j} + \\ & +[\beta^2\overline{v}_i + (\widehat{D}_{i,j}\overline{u}_i)]\widehat{D}_{i,j} + \beta^4 + \mathrm{i}\beta^3\mathrm{Re}\overline{w}_i + \\ & +\mathrm{i}\beta\mathrm{Re}(\widehat{D}^{(2)}_{i,j}\overline{w}_i) + \beta^2(\widehat{D}_{i,j}\overline{v}_i) + (\widehat{D}^{(2)}_{i,j}\overline{u}_i) \end{bmatrix} \tag{4.7}$$

$$\mathbf{b}_{i,j} = \begin{bmatrix} -\mathrm{iRe} & 0 \\ 0 & -\mathrm{iRe}(\widehat{D}^{(2)}_{i,j} - \beta^2) \end{bmatrix}$$

— for $i \neq j$

$$\mathbf{a}_{i,j} = \begin{bmatrix} \widehat{D}^{(2)}_{i,j} - \overline{v}_i\widehat{D}_{i,j} & 0 \\ & \\ 2\overline{u}_i\widehat{D}_{i,j} & \widehat{D}^{(4)}_{i,j} - \overline{v}_i\widehat{D}^{(3)}_{i,j} + [\beta^2\overline{v}_i + (\widehat{D}_{i,j}\overline{u}_i)]\widehat{D}_{i,j} + \\ & +[-2\beta^2 - \mathrm{i}\beta\mathrm{Re}\overline{w}_i - (\widehat{D}_{i,j}\overline{v}_i)]\widehat{D}^{(2)}_{i,j} \end{bmatrix} \tag{4.8}$$

$$\mathbf{b}_{i,j} = \begin{bmatrix} 0 & 0 \\ 0 & -\mathrm{iRe}\widehat{D}^{(2)}_{i,j} \end{bmatrix}$$

In the case of spatial approach the elements of matrixes $\mathbf{A}$ and $\mathbf{B}$ in Eq (4.2) can be written schematically

$$\mathbf{a}_{i,j} = \begin{bmatrix} \widetilde{a}_{11} & 0 & \widetilde{a}_{13} & 0 & 0 & 0 \\ 0 & I & 0 & 0 & 0 & 0 \\ \widetilde{a}_{31} & 0 & \widetilde{a}_{33} & 0 & 0 & 0 \\ 0 & 0 & 0 & I & 0 & 0 \\ 0 & 0 & 0 & 0 & I & 0 \\ 0 & 0 & 0 & 0 & 0 & I \end{bmatrix}$$

$$\mathbf{b}_{i,j} = \begin{bmatrix} \widetilde{b}_{11} & I & 0 & 0 & 0 & 0 \\ I & 0 & 0 & 0 & 0 & 0 \\ 0 & 0 & \widetilde{b}_{33} & \widetilde{b}_{34} & \widetilde{b}_{35} & \widetilde{b}_{36} \\ 0 & 0 & I & 0 & 0 & 0 \\ 0 & 0 & 0 & I & 0 & 0 \\ 0 & 0 & 0 & 0 & I & 0 \end{bmatrix} \tag{4.9}$$

where I is the identity matrix. The non-zero elements of the above matrixes are

$$\begin{aligned}
\widetilde{a}_{11} &= \widehat{D}^{(2)} - \overline{v}\widehat{D} - 2\overline{u} + \mathrm{i}\omega\mathrm{Re} \\
\widetilde{a}_{13} &= -\widehat{D}\overline{u} \\
\widetilde{a}_{31} &= 2\overline{u}\widehat{D} + 2(\widehat{D}\overline{u}) \\
\widetilde{a}_{33} &= \widehat{D}^{(4)} - \overline{v}\widehat{D}^{(3)} + [\mathrm{i}\omega\mathrm{Re} - (\widehat{D}\overline{v})]\widehat{D}^{(2)} + (\widehat{D}\overline{u})\widehat{D} + (\widehat{D}^{(2)}\overline{u}) \\
\widetilde{b}_{11} &= \mathrm{iRe}\overline{w} \\
\widetilde{b}_{33} &= \mathrm{iRe}[\overline{w}\widehat{D}^{(2)} - (\widehat{D}^{(2)}\overline{w})] \\
\widetilde{b}_{34} &= 2\widehat{D}^{(2)} - \overline{v}\widehat{D} - (\widehat{D}\overline{v}) + \mathrm{i}\omega\mathrm{Re} \\
\widetilde{b}_{35} &= -\mathrm{iRe}\overline{w} \\
\widetilde{b}_{36} &= -1.0
\end{aligned} \tag{4.10}$$

The generalised eigenvalue problem is solved using the NAG FORTRAN LIBRARY procedure.

In the majority of instability analyses the temporal approach is used, which gives efficiently and precisely the neutral loop and critical parameters. The spatial approach (numerically far more expensive), is used rarely, however, the results obtained by means of the spatial theory can be directly compared with the experimental results. Additionally, the spatial amplification rates are necessary for the transition prediction method $\exp(N)$. According to Gaster's transformation, it is possible to convert temporal to the spatial amplification rate using the group velocity, which represents the velocity at which energy propagates in the conservative system. However, Gaster's transformation is very accurate only near the neutral curves and when the amplification rate of disturbances becomes greater, the spatial theory results should be used to compare with the experimental results.

5. Results

The linear stability equations (3.10) have been solved using the spectral collocation method. The calculations have been made with $N = 64$ number of collocation points and with the following grid parameters $Y_{max} = 100.0$ and $Y_0 = 0.4$. The number of collocation points was chosen to obtain the maximum accuracy of calculations simultaneously not being much time-consuming. The grid refinement history and comparison with the results of the same analysis carried out by Hall et al. (1984), who used the Euler-Macluren compact scheme

for calculations are shown in Table 1 (Hall's results are indicated by *). The calculations presented in Table 1 were made for the neutral point at a lower branch for $\mathrm{Re} = 800$, $\kappa = 0$.

Table 1. The grid refinement history of the numerical solution to the eigenvalue problem

N^*	β^*	ω_r^*	N	β	ω_r
10	0.3300581	0.1226919	32	0.3381432	0.1269065
20	0.3378719	0.1267951	64	0.3384637	0.1270973
40	0.3384238	0.1270776	100	0.3384639	0.1270976
80	0.3384613	0.1270965	140	0.3384638	0.1270976
60	0.3384638	0.1270977			

From the above comparison in can be seen that, to obtain the results of comparable accuracy using the spectral collocation method we needed 64 points, whereas calculations made by means of the Euler-Maclurin scheme (Hall et al., 1984) required 160 points.

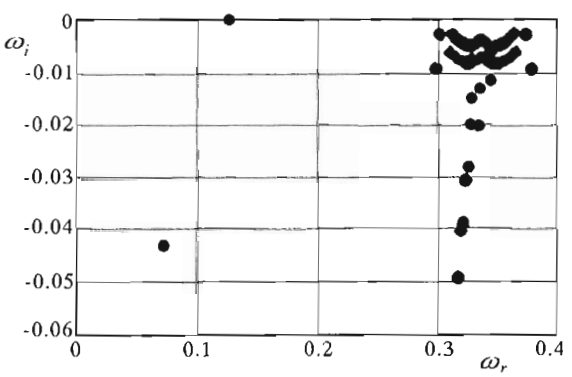

Fig. 4. Eigenvalue spectrum of the attachment-line boundary layer flow at the neutral point $\mathrm{Re} = 800$, $\kappa = 0.0$ and $\beta = 0.3384631$

The global solution method used in the present paper for solving the eigenproblem yields the full spectrum of the last damped waves. It is a much more difficult problem to obtain the whole spectrum (if possible at all) than to obtain only the most unstable wave. The most unstable mode is cut off from the spectrum, so it is relatively easy to estimate it. The full spectrum obtained at the point $\mathrm{Re} = 800$, $\kappa = 0.0$ and $\beta = 0.3384631$ we have plotted in Fig.4.

In Fig.5 we have compared between the neutral curve ($F = \omega/\mathrm{Re} = f(\mathrm{Re}_\Theta)$) obtained in the present paper for $\kappa = 0.0$ and the experimental data of Pfenninger and Bacon (1969) and Poll (1979). The line of the maximum

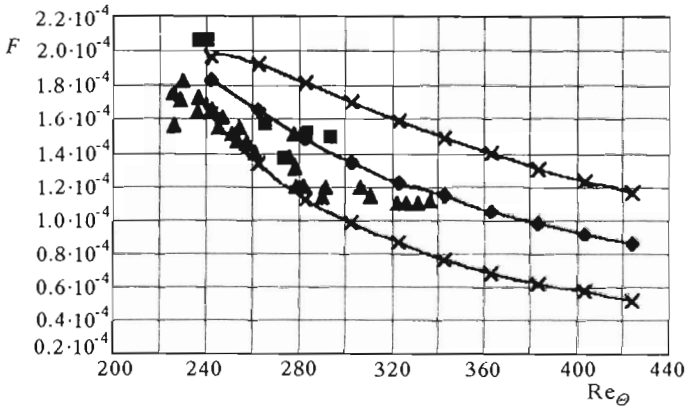

Fig. 5. Neutral curves obtained for $\kappa = 0.0$ and comparison with the experimental data of Pfenninger and Bacon (1969)

special amplification rates is marked in Fig.5. We can see that the amplified waves found by Pfenninger are located between the lower neutral branch and the line of maximum amplification rates.

Pfenninger observed also the amplified waves for the values of Reynolds number below the linear critical $\mathrm{Re}_{cr} = 583.2$ ($\mathrm{Re}_{cr} = 583.2$ was obtained in this paper, $\mathrm{Re}_{cr} = 583$ obtained by Spalart (1988), $\mathrm{Re}_{cr} = 593.1$ by Hall et al. (1984), $\mathrm{Re}_{cr} = 582$ by Powilleit (1992)) but Pfenninger's results were greater than the nonlinear critical Reynolds number $\mathrm{Re}_{cr} = 511$ found by Balakumar (1998). In Balcumar's paper the 2D, nonlinear equilibrium solutions for the swept Hiemenz flow attachment-line boundary layer are computed by solving the Navier-Stokes equations as the nonlinear eigenvalue problem.

The critical Reynolds number obtained for the Tollmien-Sclichting waves (Orr-Sommerfeld equation) for $\kappa = 0.0$ has been found of 660, whereas from the Görtler-Hammerlin formula $\mathrm{Re}_{cr} = 583.2$. Inside the unstable region, the amplification rates of the Görtler-Hammerlin disturbances are significantly greater than those of the Tollmien-Schlichting form.

Fig.6 presents the transition Reynolds number Re_{Θ_T} calculated from $\exp(n)$ method for total applification rate $n = -\int_0^{Z_T} \beta_i \, dZ = 6$ and 10 as a function of the spanwise distance Z. The results presented in Fig.6 are obtained for the Görtler-Hammerlin form of disturbances. The application of $\exp(n)$ method to the case of attachment-line is straightforward with the assumption of the uniform boundary layer from its origin to transition. In such a case Re_Θ is constant from the point A to transition (Fig.2). By applying the $\exp(n)$ rule, the transition location is $Z_T = n/(-\beta_i)_{max}$. In Fig.6 the

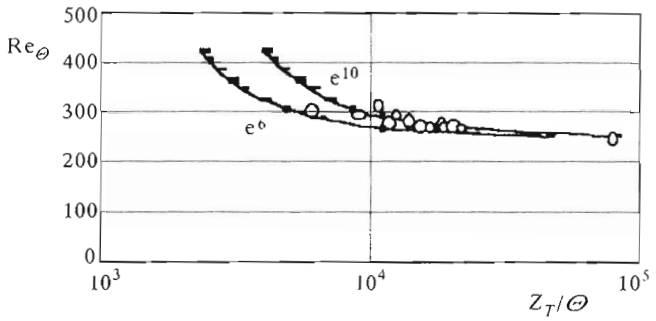

Fig. 6. Transition Reynolds number as a function of the spanwise distance Z_T/Θ

experimental data of Powilleit (1992) are presented for comparison. The experimental data are in a good agreement with our theoretical results for $n = 10$ (the agreement is particularly good for larger values of Z). Such an analysis has also been made at the maximum amplification rate $(-\beta_i)_{max}$ obtained from the Orr-Sommerfeld equation. In such a case the theoretical values for $n = 6$ are in best agreement with the experimental results.

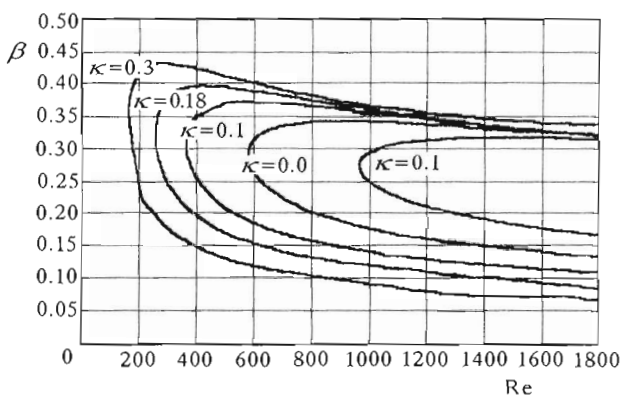

Fig. 7. Neutral curves obtained for different κ

In Fig.7 we have shown the neutral curves (wave number β as a function of the Reynolds number) obtained for the suction rates $\kappa = -0.1$, 0.0, 0.1, 0.18 and 0.3. To generate a neutral curve $(\omega_i = 0)$ we used Newton's method. The iteration process is repeated until $\omega_i = 0$ vanishes within the assumed tolerance (in the present paper $\omega_i < 10^{-5}$). It can be seen from Fig.7 that the shape of neutral curves for the flow with suction $(\kappa < 0)$ is of a viscous instability type and for blowing $(\kappa > 0)$ is of an inviscid instability and that

suction stabilises while blowing destabilises the boundary layer. The corresponding linear critical Reynolds numbers for different κ have been plotted in Fig.8. We see that the critical Reynolds number increases very rapidly with decreasing κ. In Fig.8 the obtained curve $\mathrm{Re}_{cr} = f(\kappa)$ is compared with the results of Spalart (1988) who performed direct simulation of the flow near the attachment-line of a swept cylindrical body by solving numerically (DNS) the full Navier-Stokes equations (DNS; at the limit of small perturbations). For each value of κ Spalart determined a range of the width 50 in Reynolds number in such a way that at lower Reynolds number all disturbances decayed and at higher ones at least one mode was amplified. From Fig.8 we can see that for each κ obtained in the present paper the critical Reynolds number lies within the "range".

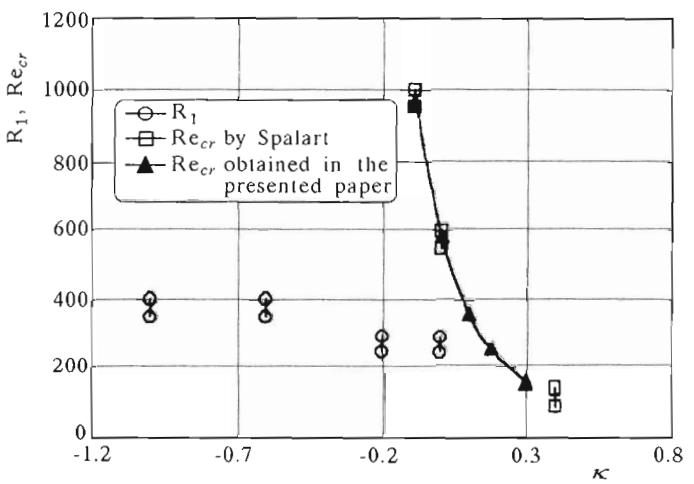

Fig. 8. Critical Reynolds number Re_{cr} versus κ and comparison with the Spalart results (R_1 and Re_{cr})

By analysing the function $\mathrm{Re}_{cr} = f(\kappa)$ one can overestimate the real stabilising influence of suction on the attachment-line boundary layer. In Fig.8 there have also shown the relaminarisation Reynolds number R_1 (the Reynolds number below which the attachment-line contamination does not arise) as a function of κ obtained by Spalart. As was done for the linear critical Reynolds number, the "range" is given for each value of κ. In this case, at the lower end, the flow was observed to relaminarise, even when the initial condition of well-developed turbulent flow was taken and at the high end of the "range", turbulence was sustained for a long time. We see that suction has a much weaker effect on R_1 than on Re_{cr}.

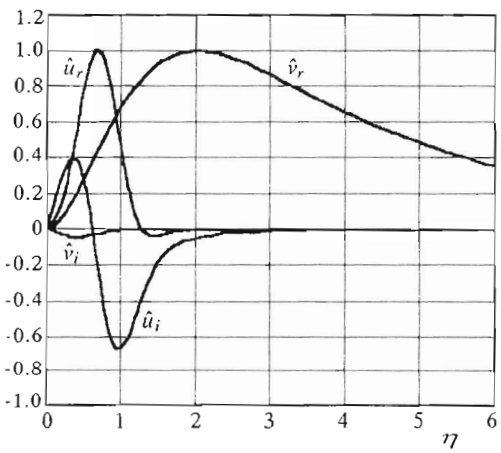

Fig. 9. Eigenfunctions corresponding to the neutral point at $\mathrm{Re} = 583$, $\beta = 0.2845$, $\kappa = 0.0$

In Fig.9 we have plotted the eigenfunctions corresponding to the neutral point at $\mathrm{Re} = 583.2$, $\beta = 0.2845$, $\kappa = 0.0$. The eigenfunctions have been normalised in each case so that the maximum of each velocity component is one. In Fig.9 we can see a rapid decrease of $\widehat{u}$ component as $Y \to \infty$, whereas $\widehat{v}$ component vanishes more slowly. This is, of course, to be expected since for large Y $\widehat{u} \sim \exp(-Y^2/2)$ and $\widehat{v} \sim \exp(-\beta Y)$ (Eq 3.14).

Agreement between the Spalart results and those obtained for the Görtler-Hammerlin form of disturbances can be also observed in Fig.9. The peak location of the rms of disturbance V' ($Y \approx 2$, at $\mathrm{Re} = 583$, $\beta = 0.2845$) obtained by Spalart agrees very well with the location of maximum of $\widehat{v}_r$ in Fig.9. Investigations conducted by Spalart (1988) proved that disturbances of the form of Eq (3.5) are most unstable and therefore most relevant in the linear stability study. This was also confirmed by Lin and Malik (1996) who studied stability of the incompressible attachment-line boundary layers by using the 2D eigenvalue approach.

To estimate accuracy of the made code we compared our results with those of Theofilis (1998) obtained by applying the linear stability theory (LST*) and the direct numerical method (DNS*; at the limit of small perturbations). The comparison made for $\mathrm{Re} = 350$ and $\kappa = 0.18$ is shown in Table 2. The comparison shows that the obtained results agree very well with those of Theofilis (LST* and DNS*).

Table 2. Comparison between the results obtained in this paper (LST) and those of Theofilis (LST* and DNS*)

	DNS*		LST*	
β	ω_r	ω_i	ω_r	ω_i
0.15625	$5.486500E-02$	$-3.4620E-03$	$5.4886E-02$	$-3.4440-03$
0.18750	$6.907600E-02$	$-1.5680E-03$	$6.9087E-02$	$-1.5500-03$
0.21875	$8.367700E-02$	$1.6300E-04$	$8.3683E-02$	$1.680-04$
0.25000	$9.857400E-02$	$1.4870E-03$	$9.8578E-02$	$1.4980-03$
0.28125	0.1136920	$2.2970E-03$	0.113695	$2.3040-03$
0.31250	0.1289580	$2.4910E-03$	0.128962	$2.4950-03$
0.34375	0.1443000	$2.0030E-03$	0.144307	$2.0030-03$
0.37500	0.1596450	$7.8200E-04$	0.159655	$7.770-04$
0.40625	0.1749130	$-1.2160E-03$	0.174928	$-1.2250-03$
0.43750	0.1900170	$-4.0280E-03$	0.190039	$-4.0420-03$

	LST	
β	ω_r	ω_i
0.15625	$5.49E-02$	$-3.44E-03$
0.18750	$6.91E-02$	$-1.55E-03$
0.21875	$8.37E-02$	$1.68E-04$
0.25000	$9.86-02$	$1.50E-03$
0.28125	0.113696	$2.30E-03$
0.31250	0.128963	$2.49E-03$
0.34375	0.144308	$2.00E-03$
0.37500	0.159656	$7.77E-04$
0.40625	0.174929	$-1.22E-03$
0.43750	0.190039	$-4.04E-03$

6. Conclusions

The linear, non-parallel stability analyses of the swept attachment-line flow were performed by studying particular three-dimensional disturbances (Görtler-Hammerlin formula). The linear stability theory equations (temporal and spatial approach) were solved by means of the spectral collocation method. The global solution method used for solving the eigenproblem yielded

the full spectrum of the least damped waves, not only the most unstable wave. Calculations were made for the boundary layer with suction and blowing. The results demonstrated strong stabilising influence of suction on the critical Reynolds number, however, the Spalart DNS results showed that suction has a much weaker effect on the relaminarisation Reynolds number. To estimate accuracy of the algorithm used in the present work we made a comparison between the instability results obtained by different authors using different approaches. The comparison showed that the results obtained in the present paper for the Görtler-Hammerlin form of disturbances are in very good agreement with the linear stability results of Hall et al. (1984), Theofilis (1998, 1995), Powilleit (1992) and with DNS of Theofilis (1998) and with DNS results of Spalart (1988) (DNS at the limit of small perturbations). We have shown that the range of frequencies of unstable waves measured by Pfenninger and Bacon (1969) and Poll (1979) corresponds to the neighbourhood of the line of maximally amplified disturbances and that the theoretically obtained transition Reynolds numbers Re_{Θ_T} (according to $\exp(n)$ method) are correlated well for the total amplification rate $n = 10$ with the experimental results of Powilleit (1992).

Finally, we would like to make a few comments about the planed extension of the presented instability work to the nonlinear calculations within the frame of the Görtler-Hammerlin form of disturbances. The X-dependence structure of disturbances will enable us to find a solution of the nonlinear stability equations by solving ordinary differential equations. Such non-linear calculations might help to understand the origin of the subcritical equilibrium disturbances measured by Pfenninger and Bacon (1969).

Acknowledgement

Authors are grateful to Dr V. Theofilis from DLR in Goettingen for consultations. The study was supported by the State Committee for Scientific Research in the frame of grant No. 7T071700317. The computations are performed on the Cray J916 at Poznań Computer Center.

References

1. BALAKUMAR P., 1998, Finite Amplitude Stability of Attachment-Line Boundary Layer, *AIAA Paper*, 98-0338

2. BERTOLOTTI F., 1999, On the Connection Between the Attachment-Line and

Crossflow Instability, *IUTAM Laminar Turbulent Transition Symposium*, Sedona, AZ

3. CANUTO C., HUSSAINI M., QUARTERONI A., ZANG T., 1988, *Spectral Methods in Fluid Dynamics*, Springer
4. HERBERT T., 1977, Finite Amplitude Stability of Plane Parallel Flows, *AGARD CP*, 224:3-1-3-10
5. HALL P., MALIK M., POLL D., 1984, On the Stability of an Infinite Swept Attachment Line Boundary layer, *Proc. Roy. Soc. Lond.*, A395, 229-245
6. GASTER M., 1967, On the Flow Along Swept Leading Edges., *Aero. Q.*, **18**, 5, 165-184
7. GÖRTLER H., 1955, Dreidimensionale Instabilität der ebenen Staupunktströmung gegenüber wirbekartigen Störungen, In *50 Jahre Grenzschichtforschung*, H. Görtler and W. Tollmien, edit., 304, Vieweg, Braunschweig
8. HAMMERLIN G., 1955, Zur instabilitatstheorie der ebenen Staupunktstromung, In *50 Jahre Grenzschichtforschung*, edit. H. Görtler and W. Tollmien, 315-327, Vieweg und Sohn
9. LIN R., MALIK M., 1996, On the Stability of Attachment-Line Boundary Layers. Part 1. The Incompressible Swept Hiemenz Flow, *J. Fluid Mech.*, **311**, 239-255
10. MALIK M., BECKWITH T., 1988, Stability of Supersonic Boundary Layer Along a Swept Leading Edge, *AGARD*, CP-438, 3-1
11. PFENNINGER W., BACON J., 1969, Amplified Laminar Boundary Layer Oscillations and Transition At the Front Attachment Line of a 45 Swept Flat-Nosed Wing with and Without Suction, In *Viscous Drag Reduction*, edit. C.S. Wells, 85-105, Plenum Press
12. POLL D., 1979, Transition in the Infinite Swept Attachment Line Boundary Layer, *Aero. Q.*, **30**, 607-629
13. POLL D., 1985, Some Observations of the Transition Process on the Windward Face of a Long Yawed Cylinder, *J. Fluid. Mech.*, **150**, 329-356
14. POWILLET G., 1992, CERT/ONERA Internal Report
15. ROSENHEAD L., 1963, *Laminar Boundary Layer*, Oxford University Press, Oxford
16. SPALART P., 1988, Direct Numerical Study of Leading-Edge Contamination, *AGARD-CP*, **438**, 5.1-5.13
17. THEOFILIS V., 1995, Spatial Stability of Incompressible Attachment-Line Flow, *Theoret. Comput. Fluid Dynamics*, **7**, 159-171
18. THEOFILIS V., 1998, On Linear and Non-Linear Instability of the Incompressible Swept Attachment-Line Boundary Layer, *J. Fluid Mech.*, **355**, 193-227

Stabilność nieściśliwej warstwy przyściennej na skośnej krawędzi natarcia

Streszczenie

Stateczność warstwy przyściennej skośnej krawędzi natarcia badana jest w pracy za pomocą liniowej teorii niestabilności. Równania liniowej teorii niestabilności wraz z warunkami brzegowymi tworzą uogólnione zagadnienie własne, które rozwiązywane jest metodą spektralnej kolokacji. Analiza stateczności została przeprowadzona dla przepływów z odsysaniem i wydmuchiwaniem. Uzyskiwane rezultaty porównywano z wynikami teoretycznymi innych autorów oraz z wynikami badań eksperymentalnych.

Manuscript received June 29, 1999; accepted for print February 18, 2000